(12) INTERNATIONAL APPLICATION PUBLISHED UNDER THE PATENT COOPERATION TREATY (PCT)

(19) World Intellectual Property Organization
International Bureau

(43) International Publication Date
03 May 2018 (03.05.2018)

WIPO | PCT

(10) International Publication Number
WO 2018/078514 A1

(51) International Patent Classification:
C01B 32/22 (2017.01) *C01B 32/194* (2017.01)

(21) International Application Number:
PCT/IB2017/056577

(22) International Filing Date:
23 October 2017 (23.10.2017)

(25) Filing Language: English

(26) Publication Language: English

(30) Priority Data:
62/412,659 25 October 2016 (25.10.2016) US

(71) Applicant: **KING ABDULLAH UNIVERSITY OF SCIENCE AND TECHNOLOGY** [SA/SA]; 4700 King Abdullah University of Science and Technology, Thuwal, 23955-6900 (SA).

(72) Inventors: **MANSOUR, Ahmed Esam**; 4700 King Abdullah University of Science and Technology, Thuwal, 23955-6900 (SA). **AMASSIAN, Aram**; 4700 King Abdullah University of Science and Technology, Thuwal, 23955-6900 (SA).

(81) Designated States *(unless otherwise indicated, for every kind of national protection available)*: AE, AG, AL, AM, AO, AT, AU, AZ, BA, BB, BG, BH, BN, BR, BW, BY, BZ, CA, CH, CL, CN, CO, CR, CU, CZ, DE, DJ, DK, DM, DO, DZ, EC, EE, EG, ES, FI, GB, GD, GE, GH, GM, GT, HN, HR, HU, ID, IL, IN, IR, IS, JO, JP, KE, KG, KH, KN, KP, KR, KW, KZ, LA, LC, LK, LR, LS, LU, LY, MA, MD, ME, MG, MK, MN, MW, MX, MY, MZ, NA, NG, NI, NO, NZ, OM, PA, PE, PG, PH, PL, PT, QA, RO, RS, RU, RW, SA, SC, SD, SE, SG, SK, SL, SM, ST, SV, SY, TH, TJ, TM, TN, TR, TT, TZ, UA, UG, US, UZ, VC, VN, ZA, ZM, ZW.

(84) Designated States *(unless otherwise indicated, for every kind of regional protection available)*: ARIPO (BW, GH, GM, KE, LR, LS, MW, MZ, NA, RW, SD, SL, ST, SZ, TZ, UG, ZM, ZW), Eurasian (AM, AZ, BY, KG, KZ, RU, TJ, TM), European (AL, AT, BE, BG, CH, CY, CZ, DE, DK, EE, ES, FI, FR, GB, GR, HR, HU, IE, IS, IT, LT, LU, LV, MC, MK, MT, NL, NO, PL, PT, RO, RS, SE, SI, SK, SM, TR), OAPI (BF, BJ, CF, CG, CI, CM, GA, GN, GQ, GW, KM, ML, MR, NE, SN, TD, TG).

Declarations under Rule 4.17:
— *as to applicant's entitlement to apply for and be granted a patent (Rule 4.17(ii))*
— *of inventorship (Rule 4.17(iv))*

Published:
— *with international search report (Art. 21(3))*

(54) **Title:** COMPOSITIONS AND METHODS OF FORMING HYBRID DOPED FEW-LAYER GRAPHENE

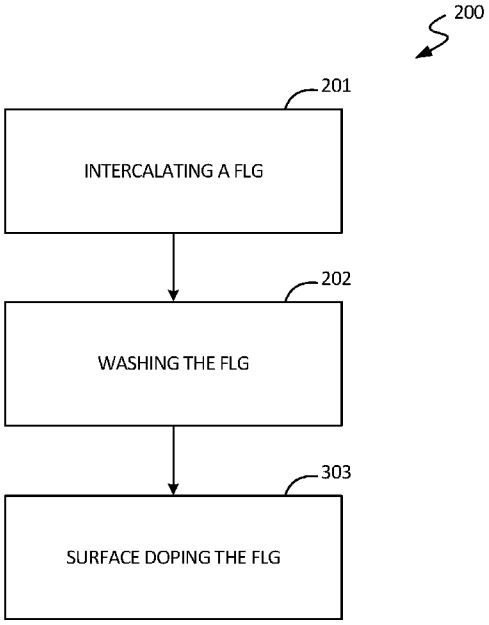


FIG. 2B

(57) **Abstract:** Embodiments of the present disclosure describe a hybrid doped few-layer graphene composition comprising an intercalant dopant in a bulk layer of a few-layer graphene and a surface dopant on a surface layer of the few-layer graphene. Embodiments of the present disclosure further describe a method of forming a hybrid doped few-layer graphene comprising intercalating a bulk layer of a few-layer graphene with an intercalant dopant, surface doping at surface layer of the few-layer graphene with a surface dopant, and washing the few-layer graphene with a solution. Embodiments also describe a transparent conducting electrode comprising a few-layer graphene, wherein the few-layer graphene comprises a bulk layer including an intercalant dopant and a surface layer including a surface dopant.

WO 2018/078514 A1

COMPOSITIONS AND METHODS OF FORMING HYBRID DOPED FEW-LAYER GRAPHENE

BACKGROUND

[0001] Molecular surface doping of single-layer graphene (SLG) and few-layer graphene (FLG) utilize molecular surface dopants that undergo charge transfer with graphene to improve conductivity. However, the improved conductivity of such surface-doped graphene is insufficient as the conductivity still falls below minimum industrial standards for transparent conducting electrode (TCE) applications. Moreover, surface doped SLG and FLG suffer from limitations with respect to carrier density, sheet resistance, and carrier mobility, among other things. In addition, the molecular surface dopants are not only exposed, but also vulnerable to the surrounding environment, which severely limits the long-term stability of doped graphene-based TCE.

SUMMARY

[0002] In general, embodiments of the present disclosure describe hybrid doped few-layer graphene compositions and methods of forming hybrid doped few-layer graphene compositions.

[0003] Accordingly, embodiments of the present disclosure describe a hybrid doped few-layer graphene composition comprising an intercalant dopant in a bulk layer of a few-layer graphene and a surface dopant on a surface layer of the few-layer graphene.

[0004] Embodiments of the present disclosure further describe a method of forming a hybrid doped few-layer graphene comprising intercalating a bulk layer of a few-layer graphene with an intercalant dopant and surface doping of a surface layer of the few-layer graphene with a surface dopant.

[0005] The details of one or more examples are set forth in the description below. Other features, objects, and advantages will be apparent from the description and from the claims.

BRIEF DESCRIPTION OF DRAWINGS

[0006] This written disclosure describes illustrative embodiments that are non-limiting and non-exhaustive. In the drawings, which are not necessarily drawn to scale, like numerals describe substantially similar components throughout the several views. Like numerals having different letter suffixes represent different instances of substantially similar components. The drawings illustrate generally, by way of example, but not by way of limitation, various embodiments discussed in the present document.

[0007] Reference is made to illustrative embodiments that are depicted in the figures, in which:

[0008] **FIG. 1** is a schematic diagram of a hybrid doped few-layer graphene with an intercalant dopant substantially present in the bulk layers of the few-layer graphene and ions of a surface dopant substantially present on a surface layer of the few-layer graphene, according to one or more embodiments of the present disclosure.

[0009] **FIG. 2A** is a schematic diagram of the process of forming a hybrid doped few-layer graphene, according to one or more embodiments of the present disclosure.

[0010] **FIG. 2B** is a flow chart of a method of forming a hybrid doped few-layer graphene, according to one or more embodiments of the present disclosure.

[0011] **FIGS. 3A-3B** are X-ray photoelectron spectroscopy (XPS) spectra in which the number of detected electrons is plotted against binding energy (eV) for hybrid doped few-layer graphene including hybrid A1 with $FeCl_3$ as the intercalant dopant and Magic Blue as the surface dopant (**FIG. 3A**) and hybrid A2 with Br_2 as the intercalant dopant and Magic Blue as the surface dopant (**FIG. 3B**), according to one or more embodiments of the present disclosure.

[0012] **FIGS. 3C-3D** are high-resolution XPS spectra of core level C 1s peak for pristine, intercalated, and hybrid doped few-layer graphene for hybrid A1 (**FIG. 3C**) and hybrid A2 (**FIG. 3D**), according to one or more embodiments of the present disclosure.

[0013] **FIGS. 4A-4D** are angle-resolved XPS spectra for hybrid A1 (**FIG. 4A**), hybrid A2 (**FIG. 4B**), few-layer graphene intercalated with $FeCl_3$ (**FIG. 4C**), and few-layer graphene intercalated with Br_2 (**FIG. 4D**), with the electron take-off angle (θ) shown on the x-axis determining the surface sensitivity of the measurement and wherein smaller values indicate increasingly surface sensitive spectra as indicated by the arrow, according to one or more embodiments of the present disclosure.

[0014] **FIGS. 5A-5C** are Raman spectra of pristine and intercalated few-layer graphene with either Br_2 or $FeCl_3$ (**FIG. 5A**), with changes of the Raman shift of the G-peak components (**FIG. 5B**), and the 2D-peak low energy component for intercalated and hybrid doped few-layer graphene (**FIG. 5C**), according to one or more embodiments of the present disclosure.

[0015] **FIGS. 6A-6C** are graphical views of various electrical transport properties of the hybrid doped few-layer graphene, including sheet resistance (**FIG. 6A**), sheet carrier density (**FIG. 6B**), and carrier mobility (**FIG. 6C**) for pristine, few-layer graphene surface doped with Magic Blue, and few-layer graphene intercalated with either $FeCl_3$ or Br_2 and hybrid doped few-layer graphene, according to one or more embodiments of the present disclosure.

[0016] **FIGS. 7A-7F** are photoelectron spectroscopy in air spectra and the deduced work function for pristine few-layer graphene (**FIG. 7A**), Br_2 intercalated few-layer graphene (**FIG. 7B**), hybrid A2 doped few-layer graphene (**FIG. 7C**), $FeCl_3$ intercalated few-layer graphene (**FIG. 7D**), hybrid B1 few-layer graphene (**FIG. 7E**), and hybrid A1 doped few-layer graphene (**FIG. 7F**), according to one or more embodiments of the present disclosure.

[0017] **FIGS. 8A-8B** are graphical views of changes in work function and shifts of the sp^2 carbon peak from XPS C 1s core level for hybrid A1 doped few-layer graphene (**FIG. 8A**) and hybrid A2 doped few-layer graphene (**FIG. 8B**), according to one or more embodiments of the present disclosure.

[0018] **FIGS. 9A-9D** are schematic views of hybrid doping of hybrid C1 (**FIG. 9A**) and hybrid D1 (**FIG. 9B**), as well as graphical views of the sheet resistance of $FeCl_3$ intercalated few-layer graphene treated with surface n-dopants for hybrid C1 (**FIG. 9C**) and hybrid D1 (**FIG. 9D**), according to one or more embodiments of the present disclosure.

[0019] **FIGS. 10A-10B** are graphical views of Hall effect measurements on hybrid C1 few-layer graphene with carrier density (**FIG. 10A**) and carrier mobility (**FIG. 10B**), according to one or more embodiments of the present disclosure.

[0020] **FIGS. 11A-11C** are photoelectron spectroscopy in air spectra and the deduced work function for $FeCl_3$ intercalated few-layer graphene (**FIG. 11A**), hybrid C1 doped few-layer graphene (**FIG. 11B**), and hybrid D1 doped few-layer graphene (**FIG. 11C**), according to one or more embodiments of the present disclosure.

DETAILED DESCRIPTION

[0021] The invention of the present disclosure relates to hybrid doping of few-layer graphene compositions and methods of forming hybrid doped few-layer graphene compositions. In particular, the invention of the present disclosure relates to hybrid doped few-layer graphene compositions formed by intercalating bulk layers of a few-layer graphene with an intercalant dopant and surface doping a surface layer of the few-layer graphene with a surface dopant. The intercalant dopants are substantially present in the bulk layers of the few-layer graphene and the surface dopants are substantially present on the surface layers of the few-layer graphene. The intercalant dopants and surface dopants may be selected to enhance an overall conductivity and tune the work function of the few-layer graphene sufficient to meet and/or exceed industrial standards for transparent conductive electrode (TCE) applications. In this way, the optoelectronic properties and work function of graphene-based TCEs may be tuned to meet specific requirements for a broad range of applications.

Definitions

[0022] The terms recited below have been defined as described below. All other terms and phrases in this disclosure shall be construed according to their ordinary meaning as understood by one of skill in the art.

[0023] As used herein, "contacting" refers to the act of touching, making contact, or of bringing to immediate or close proximity, including at the cellular or molecular level, for example, to bring about a physiological reaction, a chemical reaction, or a physical change, e.g., in a solution, in a reaction mixture, *in vitro*, or *in vivo*. Accordingly, treating, tumbling, vibrating, shaking, mixing, and applying are forms of contacting to bring two or more components together.

[0024] As used herein, "intercalating" and "surface doping" refers to depositing, chemical vapor deposition, two-zone vapor transport processing, vapor exposing, dipping, doping, etching, epitaxy, thermal oxidation, sputtering, casting, coating, dipping, submerging, spin-coating, evaporating, applying, treating, and any other technique and/or method known to a person skilled in the art.

[0025] As used herein, "washing" refers to contacting with a solution. For example, washing may refer to contacting a few-layer graphene with a solution. The few-layer graphene may be one or more of pristine, doped, undoped, partially doped, intercalated, not intercalated, and partially intercalated. Washing may be used, for example, to remove

unreacted, weakly adsorbed, and/or excess dopants (e.g., intercalant dopants and/or surface dopants) from the few-layer graphene.

[0026] Embodiments of the present disclosure describe a hybrid doped few-layer graphene composition comprising an intercalant dopant in a bulk layer of a few-layer graphene and a surface dopant on a surface layer of the few-layer graphene. **FIG. 1** is a schematic diagram of a hybrid doped few-layer graphene with an intercalant dopant substantially present in the bulk layers of the few-layer graphene and a surface dopant substantially present on the surface layer of the few-layer graphene, according to one or more embodiments of the present disclosure.

[0027] The hybrid doped few-layer graphene may include one or more of a bulk layer, a surface layer, and a substrate (not shown). The bulk layer may include one or more graphene layers and the surface layer may include one or more graphene surfaces. In many embodiments, the few-layer graphene includes a substrate and a graphene surface, with two or more graphene layers between the substrate and the graphene surface. In some embodiments, the few-layer graphene includes a first graphene surface and a second graphene surface, with two or more graphene layers between the first graphene surface and the second graphene surface. In other embodiments, any combination of substrates, graphene layers, and graphene surfaces may be utilized to form the few-layer graphene.

[0028] The few-layer graphene may be grown via chemical vapor deposition or it may be mechanically exfoliated. The few-layer graphene may be grown on any metal (e.g., nickel). In many embodiments, the few-layer graphene is grown via chemical vapor deposition. In an embodiment, once the few-layer graphene is grown, it is transferred to a substrate before one or more of intercalating and surface doping of the few-layer graphene.

[0029] The few-layer graphene may be intercalated with an intercalant dopant in the bulk layer and surface doped with a surface dopant on a surface layer. The intercalant dopant may be intercalated on one or more graphene layers in the bulk layer to form one or more layers comprising the intercalant dopant, or intercalate layer. In some embodiments, the intercalant dopant may include one or more of Br_2 and $FeCl_3$ for p-doping the bulk layer(s). In other embodiments, the intercalant dopant may include any of a large number of elements, molecules, and compounds. Intercalant dopants may be classified as acceptors and/or donors. The intercalant dopant may include one or more of alkaline earth metals, lanthanides, metal alloys, and alkali metals. The intercalant dopant may include, for example, alkali metal compounds with K, Rb, Cs, and Li. The intercalant dopant may include one or more of AsF_5

and SbF_5. The intercalant dopant may include a ternary donor intercalation compound including alkali metals with hydrogen or polar molecules (e.g., ammonia and tetrahydrofuran) and aromatic molecules (e.g., benzene). Acceptors may include one or more of compounds based on Lewis acid intercalants such as Br_2 or halogen mixtures, metal chlorides, bromides, fluorides, oxyhalides, acidic oxides such as N_2O_5 and SO_3 and strong Bronsted acids such as H_2SO_4 and HNO_3. The intercalant dopants provided herein shall not be limiting and shall include any intercalant known in the art.

[0030] The surface dopant may be surface doped on one or more graphene surfaces of the surface layer to form one or more layers comprising the surface dopant. The surface dopant may include one or more of tris(4-bromophenyl)ammoniumyl hexachloroantimonate ("Magic Blue") and molybdenum tris(1-(trifluoroacetyl)-2-(trifluoromethyl)ethane-1,2-dithiolene) ("Mo-tfd-$COCF_3)_3$") for p-doping the surface layer. The surface dopant may include one or more of ruthenium (pentamethylcyclopentadienyl)(mesitylene) dimer ("$(RuCp^*mes)_2$") and pentamethylrhodocene dimer ("$(RhCp^*Cp)_2$") for n-doping the surface layer. Any combination of the intercalant dopants and the surface dopants may be used to form the few-layer graphene. Any of a large number of other surface dopants not provided above may be utilized in any of the embodiments of the present disclosure. The surface dopants provided herein shall not be limited and shall include any surface dopant known in the art.

[0031] The intercalant dopant may form stage-*n* intercalation compounds, where *n* is generally the number of graphite layers between adjacent intercalate layers. In some embodiments, the intercalant dopant may form one or more of a stage-1 intercalation compound and a stage-2 intercalation compound. In embodiments where a stage-1 intercalation compound is formed, the bulk layer includes alternating layers of an intercalant layer and a graphene layer. In embodiments where a stage-2 intercalation compound is formed, the bulk layer includes alternating layers of an intercalant layer and two graphene layers, with no intercalant dopants present between the two graphene layers. Embodiments with a stage-1 intercalation compound generally enhance the electronic transport and optoelectronic properties of the few-layer graphene to a greater degree than embodiments with a stage-2 intercalation compound because the stage-1 intercalation compound includes a larger number of graphene layers doped with the intercalant dopant. In other embodiments, the intercalant dopant may form any stage-*n* intercalation compounds, where *n* in these embodiments is greater than 2.

[0032] The intercalant dopant and surface dopant may be compartmentalized in the bulk layer and the surface layer, respectively. For example, the intercalant dopant may be substantially present in the bulk layer and/or exclusively present in the bulk layer (e.g., not present on the surface layer). The surface dopant may be substantially present on the surface layer and/or exclusively present on the surface layer (e.g., not present in the bulk layer). In many embodiments, the intercalant dopant is substantially present in the bulk layer and the surface dopant is substantially present on the surface layer. In this way, the present disclosure provides unprecedented control over the fabrication of hybrid doped few-layer graphene to enhance electrical transport and optoelectronic properties. In particular, by compartmentalizing the intercalant dopant in the bulk layer and the surface dopant on the surface layer, the hybrid doped few-layer graphene of the present disclosure may prevent and/or preclude the two dopants from interacting chemically or otherwise in an unfavorable way. In other embodiments, the intercalant dopant may be substantially and/or exclusively present in the bulk layer and the surface dopant may be substantially and/or exclusively present on the surface layer.

[0033] The intercalant layers may provide various structural benefits to the hybrid doped few-layer graphene. For example, the presence of the intercalant dopants enhances the long-term stability of the hybrid doped few-layer graphene relative to, for example, conventional molecular surface doping of single-layer graphene and few-layer graphene, as well as conventional transparent conducting electrodes. In particular, as the number of intercalant layers present in the hybrid doped few-layer graphene increases, the long-term stability of the hybrid doped few-layer graphene improves. For instance, the long-term stability of a stage-1 intercalation compound may be greater than the long-term stability of a stage-2 intercalation compound. The long-term stability of a stage-2 intercalation compound may be greater than conventional molecular surface doped single-layer graphene, few-layer graphene, and conventional transparent conducting electrodes.

[0034] The hybrid doped few-layer graphene achieves an extremely high carrier density and an increase in overall conductivity relative to, for example, conventional molecular surface doping of single-layer graphene and few-layer graphene, as well as conventional transparent conducting electrodes. The intercalation maximizes the number of graphene layers doped in the bulk layer and eliminates electronic coupling between graphene sheets. In this way, the individually doped graphene layers may act as parallel channels of charge carriers and decrease sheet resistance to unprecedented levels to increase an overall

conductivity of the hybrid doped few-layer graphene. The surface doping further increases overall conductivity by contributing to an increase in carrier density due to additional charge transfer with surface dopants. The bulk layer screens Coulomb scattering of charged molecules from the surface layer and thus provides the added benefit of minimizing any decrease in carrier mobility that would occur due to Coulomb scattering.

[0035] Intercalating and surface doping to form the hybrid doped few-layer graphene tunes the work function. Generally, work function modulation occurs via two mechanisms. The first mechanism includes a shift of the Fermi level as a result of electron transfer to and/or from graphene for n-doping and p-doping, respectively. The second mechanism includes a shift of the vacuum level due to resulting surface dipoles. The ability to select from a wide range of intercalant dopants and surface dopants provides an effective route for modulating and/or tuning the work function (e.g., increasing the work function) of the hybrid doped few-layer graphene. In some embodiments, the increase in work function may be dominated by a Fermi level shift. In other embodiments, the increase in work function may be dominated by a significant surface dipole.

[0036] **FIGS. 2A** and **2B** illustrate methods of forming an intercalated and surface-doped few-layer graphene, according to one or more embodiments of the present disclosure. **FIG. 2A** illustrates a schematic diagram of a method of forming a hybrid doped few-layer graphene. In particular, a pristine few-layer graphene is intercalated and surface doped to form the hybrid doped few-layer graphene of the present invention, according to one or more embodiments of the present disclosure. As shown in **FIG. 2A**, intercalants are encapsulated in between the graphene layers of the bulk layer of the few-layer graphene with ions from the surface dopant present on a top surface of the surface layer.

[0037] **FIG. 2B** illustrates a flowchart of a method of forming a hybrid doped few-layer graphene, according to one or more embodiments of the present disclosure. The few-layer graphene may be formed via deposition on a transition metal and then transferred to a substrate (not shown). In some embodiments, the few-layer graphene may be formed via chemical vapor deposition on nickel and transferred to a glass substrate. The few-layer graphene may be formed via any conventional method or method known in the art.

[0038] At step 201, the few-layer graphene is intercalated. In many embodiments, a bulk layer of the few-layer graphene may be intercalated with an intercalant dopant. In embodiments where $FeCl_3$ is the intercalant dopant, the few-layer graphene may be intercalated via a two-zone vapor transport process. In embodiments where Br_2 is the

intercalant dopant, the few-layer graphene may be intercalated via vapor exposure at room temperature. Any of the intercalant dopants described above and any method of intercalating may be utilized with respect to this step.

[0039] In some embodiments (not shown), a polymer material may be applied to a surface layer of the few-layer graphene prior to intercalating the few-layer graphene. The polymer material may include polydimethylsiloxane (PDMS), for example, but any polymer material may be applied to the surface layer of the few-layer graphene. The polymer material may be applied to the surface layer of the few-layer graphene to minimize and/or prevent any contact between the surface layer and the intercalant dopant and/or to minimize the likelihood of the intercalant dopant contacting and/or interacting with the surface layer. The polymer material applied to the surface layer of the few-layer graphene may include any polymer material sufficient to minimize and/or preclude any interactions, chemically or otherwise, between the surface layer and the intercalant dopant.

[0040] At step 202, the few-layer graphene is washed. In many embodiments, the few-layer graphene is washed following step 201 to remove unreacted and/or weakly adsorbed intercalant dopants from the surface layer. With the intercalant dopants encapsulated in the bulk layer of the few-layer graphene and the unreacted and/or weakly adsorbed intercalant dopants washed from the surface layer, the method may prevent and/or preclude unfavorable chemical interactions and/or reactions with the intercalant dopant and the surface dopant. In some embodiments, the few-layer graphene may be washed with one or more of water (e.g., deionized water) and an alcohol (e.g., ethanol). The substance utilized to wash the few-layer graphene may include any suitable substance sufficient to remove a particular intercalant dopant from the surface. Step 202 is optional.

[0041] At step 203, the few-layer graphene is surface doped. In many embodiments, a surface layer of the few-layer graphene may be surface doped with a surface dopant. In some embodiments, surface doping of the surface layer of the few-layer graphene may be accomplished by dipping the few-layer graphene in a solution of the surface dopant. Any of the surface dopants described above and any method of surface doping may be utilized with respect to this step.

[0042] The steps discussed herein may be performed in any order. For example, in an embodiment, the intercalating step may be performed as the first step, the washing step may be performed as the second step, and the surface doping step may be performed as the third step. In another embodiment, the surface doping step may be performed as the first step, the

washing step may be performed as the second step, and the intercalating step may be performed as the third step. In an embodiment, the washing step may be performed before and/or after each of the intercalating step and surface doping step. In addition, any additional steps described in the present application as well as any conventional steps may be performed before, after, and/or during any of the steps described herein.

[0043] Embodiments of the present disclosure further describe a transparent conducting electrode. The transparent conducting electrode may comprise a few-layer graphene, wherein the few-layer graphene comprises a bulk layer including an intercalant dopant and a surface layer including a surface dopant. Any of the few-layer graphenes, bulk layers, intercalant dopants, surface layers, and surface dopants of the present disclosure may be included here. In addition, the transparent conducting electrode may include any other additional conventional components known in the art.

[0044] The following Examples are intended to illustrate the above invention and should not be construed as to narrow its scope. One skilled in the art will readily recognize that the Examiners suggest many other ways in which the invention could be practiced. It should be understood that numerous variations and modifications may be made while remaining within the scope of the invention.

EXAMPLE 1

[0045] The following example relates to a hybrid doping strategy for CVD-grown FLG that enabled efficient doping of all the layers of the FLG through a combination of molecular surface dopants and bulk intercalation with small molecules. The chemical composition of hybrid doped FLG varied in thickness, confirming the existence of intercalants in the bulk of the films, which doped the interior graphene layers, while the surface dopants were exclusively present on the exposed FLG surface. The two doping modalities (intercalation and surface) worked in tandem in tuning the electrical transport and electronic properties of FLG. Further p-doping effect was observed after surface doping of intercalated FLG, with the intercalation dominating the enhancement in the electrical conductivity. Surface dopants further increased the work function of intercalated FLG, via surface dipole formation. At the current stage, the doping strategy exhibited tunability for increasing the work function. The hybrid doping strategy may be utilized for large-scale CVD-FLG and provides precise control over the energetics of the bulk and the surface, separately. The hybrid doped few-layer

graphene may be utilized as graphene-based TCEs in photovoltaics and optoelectronic applications.

[0046] Chemical doping of graphene is a promising route towards facilitating its use as a TCE in various applications. Most studies of chemical doping have focused on the use of surface molecular dopants, which undergo charge transfer with graphene leading to improved conductivity and a significant shift of the work function. However, the resulting conductivity is still below the industrial standards for TCE applications. In addition, the dopants are exposed at the surface, making them more prone to the surrounding environment which can jeopardize the long-term stability of the TCE. As shown in the present disclosure, FLG may be intercalated with various species leading to low sheet resistance and extremely high carrier density. The intercalation doping maximized the number of layers being doped in FLG, with the intercalants encapsulated between the graphene layers, enhancing their long-term stability. The combination of the benefits of these two doping modalities in FLG provides a facile multi-modal doping strategy (hybrid doping). FLG intercalated with Br_2 or $FeCl_3$ also doped with surface molecular dopants, leading to lower sheet resistance and larger tunability in the work function. Angle-resolved XPS was used to locate the position of the dopants being either on the surface of in the bulk. The further increase in the conductivity was attributed to the increase in the carrier density due to additional charge transfer with the surface dopants, while the mobility was not affected as evident by Hall effect measurements. The work function further increased after surface doping, which was attributed to contributions from shifts in the vacuum energy level as a result of surface dipoles resulting from the charge transfer.

[0047] FLG offered a unique platform pertinent to the modulation of the electrical and electronic properties by doping. Being amenable to intercalation of small molecules in a manner similar to GIC, allowed for effective doping of the bulk of FLG depending on the staging of the intercalate molecules, thereby achieving high carrier density on the order of 10^{15} cm^{-2}, a regime that was previously not accessible via conventional molecular surface doping of SLG and FLG. Moreover, the intercalation process eliminated the electronic coupling between graphene sheets. The improvement in overall conductivity resulted from doped individual layers acting as parallel channels for the charge carriers and a decrease in sheet resistance to values as low as 8.8 Ω/□ for mechanically exfoliated FLG. Molecular surface doping of graphene proved to be an effective route to modulate its work function, in addition to increasing the conductivity which, however, was limited by the significant

decrease in the carrier mobility due to Coulomb scattering by charged molecules (after electron transfer), an effect that was shown to be minimized in FLG due to screening of such charges by the additional layers in the bulk. Work function modulation generally occurs via two mechanisms; (1) shift of the Fermi level as a result of electron transfer to/from graphene for n- and p-doping, respectively, and (2) shift of the vacuum level due to the resulting surface dipoles. These two mechanisms may be combinedly achieved via a combination of the two doping modalities just described, namely, bulk intercalation and molecular surface doping, thus have the potential to provide larger tunability of the work function in addition to achieving low sheet resistance. CVD-FLG was p-doped through intercalation with either Br_2 or $FeCl_3$ followed by surface p-doping using tris(4-bromophenyl)ammoniumyl hexachloroantimonate "Magic Blue" and molybdenum tris(1-(trifluoroacetyl)-2-(trifluoromethyl)ethane-1,2-dithiolene) "Mo-(tfd-$COCF_3)_3$", or surface n-doping using ruthenium (pentamethylcyclopentadienyl)(mesitylene) dimer "$(RuCp^*mes)_2$" and pentamethylrhodocene dimer "$(RhCp^*Cp)_2$". Angle-resolved XPS (ARXPS) was employed to gain insights into the position of the dopants in the doped FLG. The intercalants were encapsulated beneath the surface and into the bulk layers of FLG, while the surface dopants were present only at the surface. This compartmentalized the different dopants, which do not mix unfavorably or interact chemically in any meaningful way. Systematic characterization of the electrical transport properties showed that the enhancement of the conductivity was dominated by the increase of the carrier density from ~ 3×10^{13} cm^{-2} to ~ 6×10^{14} cm^{-2}, thus compensating for the decrease in the mobility from 289 $cm^2/(Vs)$ to ~ 90 $cm^2/(Vs)$ with a significant contribution coming from the intercalant dopant. The surface dopants were observed to additionally increase the carrier density, without affecting the mobility since the related Coulomb scattering was screened by the topmost graphene layers. Accordingly, an overall increase in the conductivity was achieved using the hybrid approach with the sheet resistance dropping from ~ 863 Ω/□ to ~ 100 Ω/□. The work function was further increased with surface doping of intercalated FLG up to 5.43 eV shifting by 0.55 eV as compared to the shift of ~ 0.40 due to intercalation alone. This was due to additional contribution from the vacuum level shift due to the formation of surface dipoles from surface dopants. The hybrid doped FLGs of the present disclosure may be tuned with respect to optoelectronic properties and the work function of graphene-based TCEs to meet the specific requirements of a broad range of applications.

[0048] CVD grown FLG on nickel was transferred to a glass substrate using the PMMA transfer followed by thermal annealing procedure. The samples were first intercalated with either $FeCl_3$ using the two-zone vapor transport process for about 360 mins or Br_2 using vapor exposure at room temperature for about 180 mins (intercalated). Surface doping was then carried out by dipping the intercalated FLG (bulk-doped) in solutions of either the p-dopants Magic blue ("hybrid A") or Mo-(tfd-$COCF_3$)$_3$ ("hybrid B") or the n-dopants (RuCp*mes)$_2$ ("hybrid C") and (RhCp*Cp)$_2$ ("hybrid D") for about 60 mins.

[0049] The intercalation process was carried out as the first step to prevent potential chemical reactions with the intercalant and the surface dopants, considering the reactivity of both $FeCl_3$ and Br_2, in addition to the high-temperature processing involved in the former (about 360°C). Interaction of the surface molecular dopants was limited to the surface of graphene and thus was not expected to interact with the intercalants since they are encapsulated in between the graphene layers. See **FIG. 1**. An essential step in the doping procedure is washing the intercalated FLG to remove unreacted and weakly adsorbed intercalants from the surface so that the subsequent surface doping step may proceed without unfavorable interactions with the intercalants on the surface of FLG. $FeCl_3$-FLG was washed with DI water considering the hygroscopic nature of $FeCl_3$, and Br_2-FLG was washed with ethanol, which was demonstrated to be efficient in removing weakly adsorbed bromine from FLG surface. Br_2 may potentially bind covalently with carbon, so its presence on the surface may not be avoided in some embodiments. The formation of Br_2-carbon covalent bonds may reduce the available interaction surface for surface dopants.

Doping effect and the chemical composition of the hybrid-doped FLG

[0050] **FIG. 3A** shows survey XPS spectra of pristine, $FeCl_3$ intercalated and hybrid doped FLG with Magic Blue as the surface dopant (hybrid A1). The coexistence of bulk and surface doping was evident by the mutual appearance of Sb 4d (surface) and Fe 3p (bulk) peaks in the hybrid doped sample as shown in the inset of **FIG. 3A**. Similarly, the survey XPS spectra of Br_2 intercalated and hybrid doped FLG shown in **FIG. 3B** indicated the coexistence of bromine intercalant (Br 3d) and antimony (Sb 4d) from the surface dopant. High-resolution XPS C 1s peak shifted to a lower binding energy from 284.10 eV for pristine FLG to ~ 283.85 eV for $FeCl_3$ intercalated FLG and further to 283.70 eV once the surface dopant Magic blue was added, which was a consequence of p-doping as shown in **FIG. 3C**. Br_2 intercalated FLG exhibited a similar trend, but with smaller shifts, where the C 1s downshifted to 283.90 eV after intercalation, where it slightly shifted after surface doping as

shown in **FIG. 3D**. The further decrease in the C 1s binding energy in hybrid doped FLG indicated that surface doping can additionally p-dope the intercalated FLG and additionally lower the Fermi level. This pointed to the fact that the surface dopant increased the carrier density of intercalated FLG since the shifts in the Fermi energy were directly related to the square root of the induced charge carriers into graphene.

[0051] The larger down-shift of C 1s for the $FeCl_3$ intercalation pointed to its higher p-doping effect than Br_2, which is probably due to its ability to form stage-1 intercalation compounds with FLG and dope larger number of graphene layers, whereas bromine can only form a maximum of stage-2 intercalation compounds. This shift of the core level C 1s peak, however, was counter-intuitive to the expected upshift in the binding energy of core level peaks once they lost electrons, since the positive charge of the nucleus became less screened and thus increased its binding with the remaining core electrons.

[0052] However, such downshift was attributed to the lowering of the Fermi energy level in p-doped materials, which aligned with the Fermi energy level of the detector in photoelectron spectroscopy instrumentation, to which the XPS spectrum was referenced, as had been previously observed for p-doped graphite, carbon nanotubes, and graphene.

[0053] The atomic content of the Sb (surface dopant) gradually increased as the take-off angle decreased (increasingly surface sensitive) as shown in **FIG. 4A** for hybrid A1 and **FIG. 4B** for hybrid A2. This confirmed the exclusive existence of the molecular dopant (Magic Blue) on the surface of the intercalated FLG. However, for larger take-off angles (such as 90°), the measurements were bulk-sensitive and therefore the Sb/C atomic ratio was expected to be lower as shown in **FIGS. 4A** and **4B**. $FeCl_3$ intercalant gradually decreased with increasing surface sensitivity, where the atomic ratio of Fe with respect to C decreased as shown in **FIG. 4A**, whereas Br_2 intercalant exhibited a nearly constant atomic content at all electron take-off angles which was expected for uniformly bulk-doped FLG. A control measurement on only intercalated FLG was conducted and a similar trend in the atomic content of iron for $FeCl_3$ intercalation was observed (**FIG. 4C**). This indicated the absence of $FeCl_3$ on the surface of FLG and demonstrated the effectiveness of the washing step in the experimental procedure. Moreover, this led to the conclusion that intercalation of $FeCl_3$ was more concentrated at the bottom surface of FLG closer to the substrate and that a fully stage-1 intercalated FLG may not have been achieved, which was a limitation for the intercalation of CVD FLG due to intrinsic differences in crystallinity and layers coupling from highly oriented pyrolytic graphite (HOPG). Recent reports on $FeCl_3$ intercalated FLG demonstrated

that full intercalation could only be achieved for mechanically exfoliated FLG, which closely resembled the structure of graphite, whereas in the case of CVD FLG, non-uniform and incomplete intercalation was reported under the same processing conditions. Additionally, the trend of the atomic content of iron in **FIG. 4C** was explained by the fact that desorption of intercalant would be easier from the outer surface of the layers away from the substrate as was recently demonstrated for $FeCl_3$ intercalated FLG. On the other hand, bromine content in only Br_2 intercalated FLG shown in in **FIG. 4D** confirmed the nearly constant bromine content observed in the hybrid A2 samples, which can be contrasted to the case of $FeCl_3$ intercalated FLG by the fact bromine can potentially form covalent bonds with the basal plane of the topmost layer, and the edges of the sheets throughout the bulk. A comparison of the total amount of the surface dopant (Magic Blue) in the hybrid A1 and hybrid A2, showed that the former exhibited a higher atomic content of Sb ~5 at%, while the latter exhibited a significantly smaller amount of ~1 at%. This was expected to result from the presence of covalently Br_2 atoms on the surface and edges, which may not have been completely removed by the washing step and thus may have prevented the surface dopant from interacting with FLG. This was further confirmed by the uniform atomic content of Br with respect to carbon as a function of electron take-off angle where it slightly increased for the lowest angle (20°) indicating the presence of bromine on the surface.

[0054] **FIG. 5A** shows Raman spectra of pristine and intercalated FLG with either Br_2 or $FeCl_3$. Pristine FLG exhibited the two main peaks of graphitic materials, namely, the G-peak at ~1580 cm^{-1} originating for the in-plane stretching mode (E_{2g}) originating from the optical phonon near the Γ point, and the second order 2D-peak at ~2743 cm^{-1} arising from two optical phonons at the K point. The D-peak – which typically appears at ~1350 cm^{-1} – was activated by the presence of defects and exhibited very low intensity indicating the high quality of the graphene domains in the samples.

[0055] The shape of the 2D-peak depended on the electronic structure of graphene films and reflected the stacking order and the number of graphene layers. SLG typically exhibited a single and sharp Lorentzian peak that splits into various components in AB-Bernal stacked graphene layers until it resembles that of HOPG where it was composed of two components, with the lower energy component having approximately ¼ the intensity of the high-energy component. However, in the case of turbostratic graphite, the 2D-peak resembled the shape of that for SLG with single Lorentzian peak indicating the absence of layer coupling and resembling the electronic structure of SLG. The 2D-peak in the samples

was fitted with two Lorentzian peaks, with the lower energy component being as intense as the high energy component, which was attributed to randomly rotated stacking and agreed with previous results on epitaxially grown FLG.

[0056] Upon exposure to the intercalants, the G-peak split into a doublet as shown in **FIG. 5A**, with the lower energy peak positioned around that of the pristine FLG and originating from graphene layers not adjacent to intercalant, and a higher energy peak from intercalant bound graphene layers, the position of which was generally dependent on the degree of intercalation and the doping strength of the intercalant. Raman shifts in the low energy G-peak position are shown in **FIG. 5B**, with the inset showing the high energy G-peak shifts for intercalated and hybrid doped FLG. Both G-peak components upshifted with intercalation and the subsequent hybrid doping, which was a signature of doped graphene. The shift was larger in the case of $FeCl_3$ intercalation, indicating a larger doping effect due to its ability to intercalate into each interlayer spacing in FLG (stage 1). This was in agreement with XPS results of the higher atomic content of iron as compared to bromine in **FIG. 2** and the larger downshifts of C 1s peaks in the case of $FeCl_3$ intercalation (**FIG. 3).** Furthermore, the upshift of both components of the G-peak continued to increase upon adding the surface dopant to intercalated FLG as shown in **FIG. 5B**. The same trend was observed for the low energy fitted components of the 2D-peak shown in **FIG. 5C**, which was more sensitive to doping effects. The additional shifts in the Raman peaks, once the intercalated FLG was treated with the surface dopants, was in agreement with the XPS observation in that the hybrid doping approach contributed towards more efficient doping of all available layers in FLG with an additional shift in the Fermi level as reflected by the additional upshift in the Raman G- and 2D-peaks.

[0057] The upshift in the G-peak was observed for doped graphene, reflecting the changes in the Fermi energy level and results from the non-adiabatic removal of the Kohn anomaly at the Γ point in addition to changes in the lattice constant where it contracts in the case of electron removal in p-doping and thus stiffens the phonon mode or expands in the case of adding electrons in n-doping and thus softening the phonons. In the case of acceptor intercalants, these two mechanisms worked together and an overall upshift in the G-peak was always observed. On the other hand, the fact that 2D-peak originated from phonons away from the Γ point, its shifting was only attributed to the latter mechanism, where the upshift was a signature of p-doping due to phonon stiffening as a result of lattice contraction that accompanied the electron transfer away from graphene.

Electrical transport properties of hybrid-doped FLG

[0058] The sheet resistance of pristine FLG on glass was 863±81 Ω/□ as measured from linear 4-point probe. Upon intercalation with Br_2 the sheet resistance decreased to 391±13 Ω/□, which was further reduced in hybrid A2 doped FLG to 237±35 Ω/□ as shown in **FIG. 6A**. A similar trend was observed for the Hybrid A1 doped FLG where $FeCl_3$ intercalation resulted in a sheet resistance reduction to 137.6±6.4 Ω/□, which further decreased with surface doping to 100.1±3.3 Ω/□.

[0059] The sheet resistance of only surface doped sample FLG with Magic blue was 414.6±19 Ω/□, demonstrating that the combination of both surface and intercalation doping of FLG was crucial for achieving the highest electrical conductivity. However, the choice of the surface dopant was important to achieving the desirable conductivity of the doped sample, since using $Mo(tfd\text{-}COCF_3)_3$ with $FeCl_3$ intercalated FLG caused an increase in the sheet resistance to 165.38±9.3 Ω/□, since the effect of the surface dopants resulted from a balance between the injected charge carriers and the reduction of carrier mobility due to Coulomb scattering.

[0060] To elucidate the effect of the presented doping modalities on the transport properties, Hall effect measurements were conducted on the various stages towards hybrid doped FLG. **FIG. 6B** shows the changes in the carrier density, which significantly increased after $FeCl_3$ intercalation from 3.05×10^{13} cm^{-2} for pristine FLG to 4.78×10^{14} cm^{-2}, which was nearly an order of magnitude higher than the value obtained for surface doping only with Magic blue (7.98×10^{13} cm^{-2}). The effective doping of a significant number of the graphene layers in the bulk with intercalation was responsible for the high increase in the carrier density as compared to surface doping. However, for Br_2 intercalated FLG the carrier density moderately increased to 5.7×10^{13} cm^{-2}, which was consistent with the lower atomic content of bromine as compared with $FeCl_3$ as shown in **FIG. 4** due to the lower expected staging. For the hybrid doped FLG, the carrier density further increased to 5.91×10^{14} cm^{-2} for hybrid A1, whereas it increased to 8×10^{13} cm^{-2} for hybrid A2, reflecting the cumulative doping effect of both doping modalities. **FIG. 6C** shows the changes in the charge carrier mobility where it significantly reduced from the pristine FLG value of 289.1 $cm^2/(Vs)$ to 89.2 $cm^2/(Vs)$ for $FeCl_3$ intercalated FLG due to the Coulomb scattering by charged dopants and the fact that $FeCl_3$ was present throughout the bulk of the sample. The scattering effect was demonstrated to be minimal in the case of surface doped sample especially for FLG, where the charge dopant molecules (after electron transfer) were screened by the additional graphene layers in

FLG; where the mobility decreased to 196.63 $cm^2/(Vs)$ in the case of Magic Blue doped FLG as shown in **FIG. 6C**. The addition of the surface dopants to the intercalated FLG in hybrid A1 doped sample did not deteriorate the carrier mobility, which, at 91.4 $cm^2/(Vs)$, was nearly equal to that of the $FeCl_3$ intercalated FLG.

[0061] Despite the fact that the charge carrier mobility decreased by more than 65%, the carrier density observed an enormous increase by more than 1800% and thus an overall increase in the resulting conductivity was achieved for the hybrid A1 doped FLG. Bromine intercalation, however, exhibited a moderate effect on the carrier mobility, where the mobility reduced to 255.4 $cm^2/(Vs)$ upon intercalation, with a further reduction after the surface dopant was added to a value of 219.5 $cm^2/(Vs)$.

Work function shifts in hybrid-doped FLG

[0062] The effect of the various dopant modalities and their combination on the work function is shown in **FIG. 7**. The work function was measured using photoelectron spectroscopy in air (PESA), where pristine FLG exhibited a value of 4.88 eV as shown in **FIG. 7A**. Upon intercalation with bromine (**FIG. 7B**), the work function increased to 5.08 eV. For $FeCl_3$ intercalated FLG, a larger work function shift was observed, with an absolute value of 5.29 eV as shown in **FIG. 7D**. The larger increase in the work function for the case of $FeCl_3$ intercalated as compared to Br_2 agreed with the previously demonstrated XPS, Raman and Hall effect measurement results, which indicated a qualitatively larger shift in the Fermi energy level for the former. Treating intercalated FLG with surface dopants demonstrated the tunability of the hybrid few-layer graphene and an additional increase in the work function. The surface doping of Br_2-FLG with Magic Blue (hybrid A2) further increased the work function to 5.27 eV once the surface dopant magic blue was applied as shown in **FIG. 7C**. The work function corresponding to the addition of the surface molecular dopants Mo-(tfd-$COCF_3$)$_3$ (hybrid B1) and Magic blue (hybrid A1) to $FeCl_3$ intercalated FLG are shown in **FIGS. 7E** and **7F**, respectively. Hybrid B1 exhibited a moderate change in the work function of 0.05 eV whereas hybrid A1 led to a larger shift of 0.14 eV with a work function value of 5.43 eV. Such larger shifts in the latter were attributed to the larger doping strength of magic blue.

[0063] A comparison between the shifts of the Fermi level approximated from the sp^2 fitted peak in the XPS C 1s core level peaks, and the shifts in the work function obtained from PESA is shown in **FIG. 8**. The total change in the work function of graphene was due to changes in the Fermi energy level as a result of electron transfer and the changes in vacuum

level resulting from dipole formation. For $FeCl_3$ intercalation and the hybrid A1 doped FLG (**FIG. 8A**), the differences between the work function and the Fermi level shifts were always present and was an indication of significant surface dipole contribution to the total work function change.

[0064] However, in the case of Br_2 intercalated sample shown in **FIG. 8B** the shifts in the work function coincided with the shift in the Fermi energy level, where a considerable difference existed once the surface dopants were applied (hybrid A2), indicating that the additional shift came from vacuum level shifts due to the formation of surface dipoles. The presence of vacuum level shift for $FeCl_3$ intercalated sample in contrast to its absence for the Br_2 intercalated sample may be explained by the fact that the surface dipole dominated the changes in work function at large carrier density due to the linear dependence of such contribution on the carriers density (n) involved in the charge transfer (proportional to n), whereas the Fermi level shift contribution had a weaker dependence (proportional to $n^{1/2}$). Thus, the larger increase in the carrier density for $FeCl_3$ intercalation as compared to Br_2 intercalation as shown in **FIG. 5B** may lead to considerable molecular dipole buried in the bulk of FLG. For the hybrid doped FLG (A1 and A2), the additional shifts in the work function were dominated by vacuum level shift contribution, which explained the large changes in the work function as compared to the changes in the sheet carrier density.

Combining surface n-dopants with bulk p-type intercalants

[0065] Aiming to achieve a tunable work function towards a lower energy (decreasing Φ) the method implemented a hybrid doping approach using intercalated FLG with $FeCl_3$ and surface metal-organic dimers $(RuCp^*mes)_2$ (hybrid C1) and $(RhCp^*Cp)_2$ (hybrid D1), which were strong n-dopants. Schematics of these structures are shown in **FIGS. 9A** and **9B**, respectively. The sheet resistance increased significantly after applying the surface dopants as shown in **FIGS. 9C** and **9D**, where it increased from 137.6 ± 6.4 Ω/□ for $FeCl_3$ intercalated FLG to 293.9 ± 6.4 Ω/□ for hybrid C1 and to 344.6 ± 31.4 Ω/□ for hybrid D1.

[0066] Hall-effect measurement was performed on hybrid C1 to elucidate the increase in the sheet resistance. **FIG. 10A** shows that the surface dopant does not result in any increase in the carrier density, indicating the surface n-dopants are not effectively doping the intercalated FLG. In fact, the charge transfer from surface dopants was expected to decrease the carrier density since electrons may neutralize the hole doped FLG. The absence of such effects is attributed to the fact that $FeCl_3$ intercalated FLG was heavily p-doped, and thus n-doping had a minimal effect. However, exposing $FeCl_3$ intercalated FLG to surface n-dopant

$(RuCp^*mes)_2$ resulted in decreasing the carrier mobility as shown in **FIG. 10B**, where it decreased from 89.2 $cm^2/(Vs)$ for intercalated FLG to 50.3 $cm^2/(Vs)$ for hybrid C1. This reduction in the mobility was attributed to the introduction of charged molecules on the surface leading to additional Coulomb scattering.

[0067] **FIGS. 11A-11C** are photoelectron spectroscopy in air spectra and the deduced work function for $FeCl_3$ intercalated few-layer graphene (**FIG. 11A**), hybrid C1 doped few-layer graphene (**FIG. 11B**), and hybrid D1 doped few-layer graphene (**FIG. 11C**), according to one or more embodiments of the present disclosure. The work function was nearly unchanged for the hybrid C1 and D1 doped FLG, as shown in **FIGS. 11B** and **11C**, respectively. The large shift in the Fermi level resulting from p-doping of the bulk may explain the unchanged work function in hybrid doped FLG with n-doping surface molecules. The latter may shift the vacuum level to a direction that reduced the work function; however, this may be shaded by the significantly large Fermi level shift (towards increasing work function) resulting from bulk doping.

[0068] Accordingly, the hybrid doping approach of combining bulk p-dopants with surface n-dopants showed no clear benefits at this stage since the conductivity significantly decreases without resulting in a considerable shift in the work function, and thus defying the main objective of the hybrid doping approach.

[0069] Other embodiments of the present disclosure are possible. Although the description above contains much specificity, these should not be construed as limiting the scope of the disclosure, but as merely providing illustrations of some of the presently preferred embodiments of this disclosure. It is also contemplated that various combinations or sub-combinations of the specific features and aspects of the embodiments may be made and still fall within the scope of this disclosure. It should be understood that various features and aspects of the disclosed embodiments can be combined with or substituted for one another in order to form various embodiments. Thus, it is intended that the scope of at least some of the present disclosure should not be limited by the particular disclosed embodiments described above.

[0070] Thus the scope of this disclosure should be determined by the appended claims and their legal equivalents. Therefore, it will be appreciated that the scope of the present disclosure fully encompasses other embodiments which may become obvious to those skilled in the art, and that the scope of the present disclosure is accordingly to be limited by nothing other than the appended claims, in which reference to an element in the singular is not

intended to mean "one and only one" unless explicitly so stated, but rather "one or more." All structural, chemical, and functional equivalents to the elements of the above-described preferred embodiment that are known to those of ordinary skill in the art are expressly incorporated herein by reference and are intended to be encompassed by the present claims. Moreover, it is not necessary for a device or method to address each and every problem sought to be solved by the present disclosure, for it to be encompassed by the present claims. Furthermore, no element, component, or method step in the present disclosure is intended to be dedicated to the public regardless of whether the element, component, or method step is explicitly recited in the claims.

[0071] The foregoing description of various preferred embodiments of the disclosure have been presented for purposes of illustration and description. It is not intended to be exhaustive or to limit the disclosure to the precise embodiments, and obviously many modifications and variations are possible in light of the above teaching. The example embodiments, as described above, were chosen and described in order to best explain the principles of the disclosure and its practical application to thereby enable others skilled in the art to best utilize the disclosure in various embodiments and with various modifications as are suited to the particular use contemplated. It is intended that the scope of the disclosure be defined by the claims appended hereto

[0072] Various examples have been described. These and other examples are within the scope of the following claims.

WHAT IS CLAIMED IS:

1. A hybrid doped few-layer graphene composition, comprising:
an intercalant dopant in a bulk layer of a few-layer graphene; and
a surface dopant on a surface layer of the few-layer graphene.

2. The composition of claim 1, wherein the intercalant dopant forms a stage-1 intercalation compound with the few-layer graphene.

3. The composition of claim 1, wherein the intercalant dopant forms a stage-2 intercalation compound with the few-layer graphene.

4. The composition of claim 1, wherein the intercalant dopant includes one or more of alkaline earth metals, lanthanides, metal alloys, alkali metals, halides, and metal halides.

5. The composition of claim 1, wherein the intercalant dopant includes one or more of Br_2 and $FeCl_3$.

6. The composition of claim 1, wherein the surface dopant includes one or more of a surface p-dopant and a surface n-dopant.

7. The composition of claim 1, wherein the surface dopant includes one or more of tris(4-bromophenyl)ammoniumyl hexachloroantimonate, molybdenum tris(1-(trifluoroacetyl)-2-(trifluoromethyl)ethane-1,2-dithiolene), ruthenium (pentamethylcyclopentadienyl)(mesitylene) dimer, and pentamethylrhodocene dimer.

8. The composition of claim 1, wherein the few-layer graphene is grown via chemical vapor deposition.

9. A method of forming a hybrid doped few-layer graphene, comprising:
intercalating a bulk layer of a few-layer graphene with an intercalant dopant;

surface doping a surface layer of the few-layer graphene with a surface dopant; and

washing the few-layer graphene with a solution.

10. The method of claim 9, wherein intercalating includes intercalating via a two-zone vapor transport process or vapor exposure.

11. The method of claim 9, wherein the intercalant dopant includes one or more of Br_2 and $FeCl_3$.

12. The method of claim 9, wherein surface doping includes dipping in a solution of the surface dopant.

13. The method of claim 9, wherein the surface dopant includes one or more of a surface p-dopant and a surface n-dopant.

14. The method of claim 9, wherein the surface dopant includes one or more of tris(4-bromophenyl)ammoniumyl hexachloroantimonate, molybdenum tris(1-(trifluoroacetyl)-2-(trifluoromethyl)ethane-1,2-dithiolene), ruthenium (pentamethylcyclopentadienyl)(mesitylene) dimer, and pentamethylrhodocene dimer.

15. The method of claim 9, wherein washing includes contacting the few-layer graphene with a solution.

16. The method of claim 9, wherein washing includes contacting with one or more of water and ethanol.

17. The method of claim 9, wherein the washing step is performed after the intercalating step and before the surface doping step.

18. A transparent conducting electrode, comprising:

a few-layer graphene, wherein the few-layer graphene comprises:

a bulk layer including an intercalant dopant; and

a surface layer including a surface dopant.

19. The electrode of claim 18, wherein the intercalant dopant includes one or more of Br_2 and $FeCl_3$.

20. The electrode of claim 18, wherein the surface dopant includes one or more of tris(4-bromophenyl)ammoniumyl hexachloroantimonate, molybdenum tris(1-(trifluoroacetyl)-2-(trifluoromethyl)ethane-1,2-dithiolene), ruthenium (pentamethylcyclopentadienyl)(mesitylene) dimer, and pentamethylrhodocene dimer.

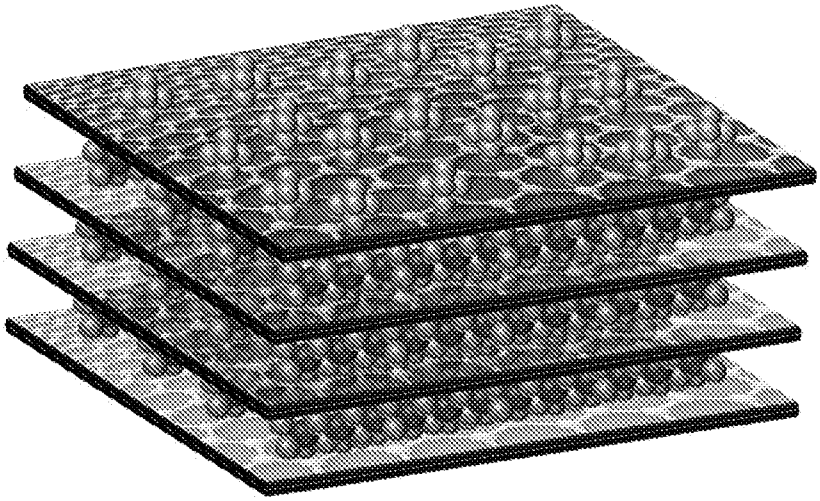


FIG. 1

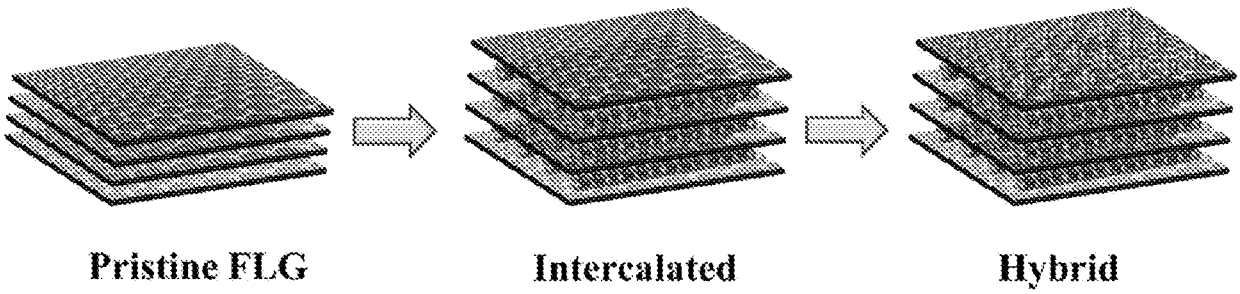


FIG. 2A

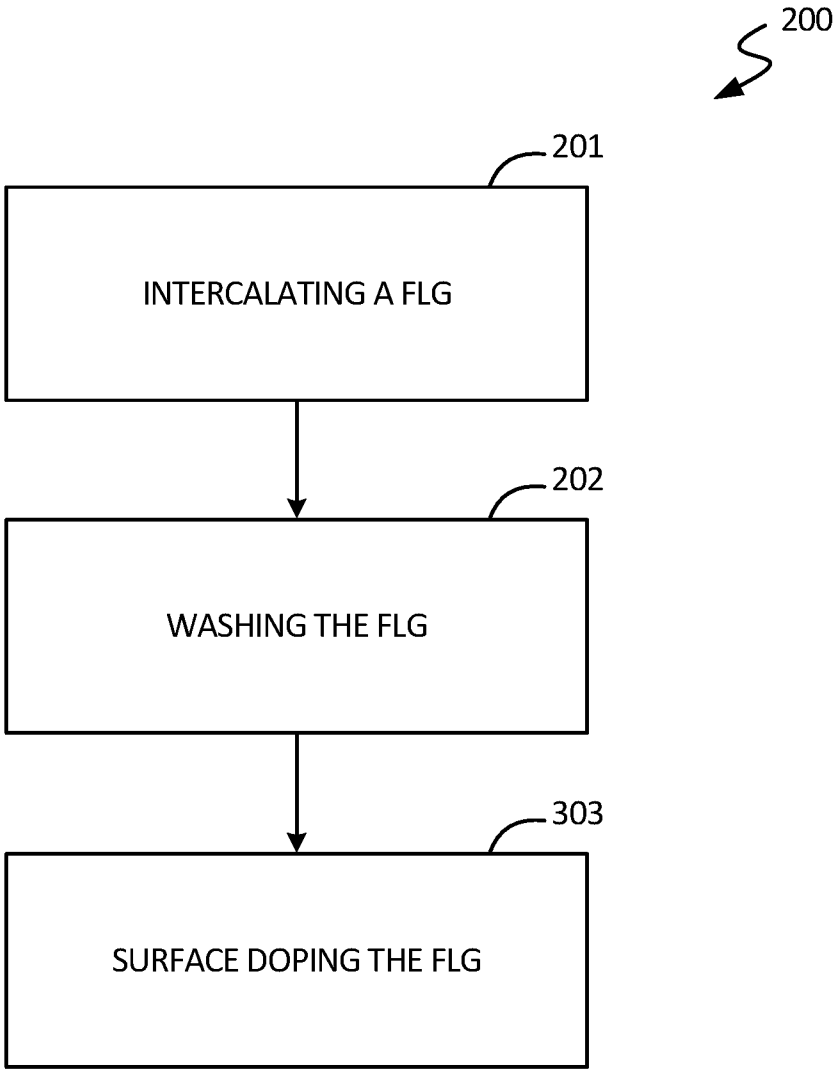

200
201
INTERCALATING A FLG
202
WASHING THE FLG
303
SURFACE DOPING THE FLG

FIG. 2B

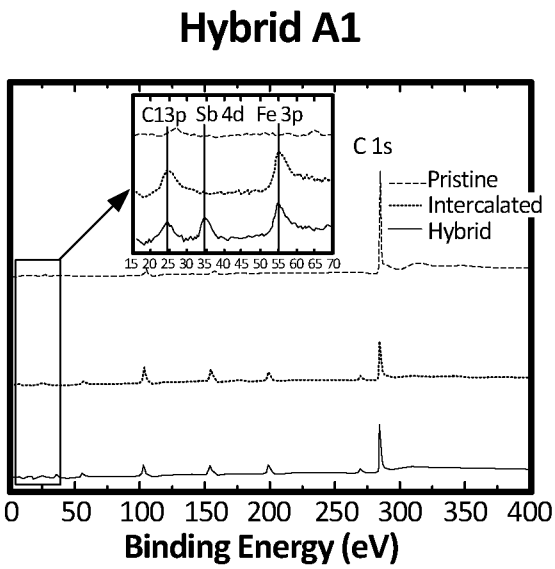


FIG. 3A

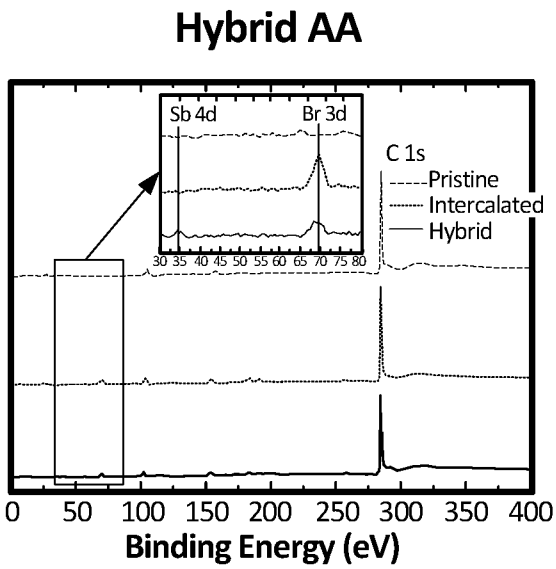


FIG. 3B

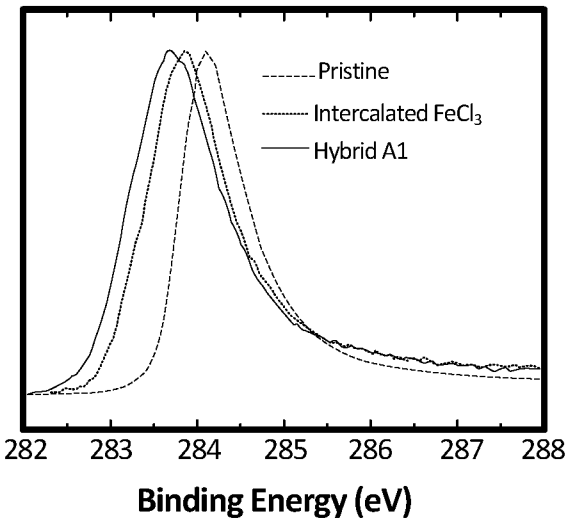


FIG. 3C

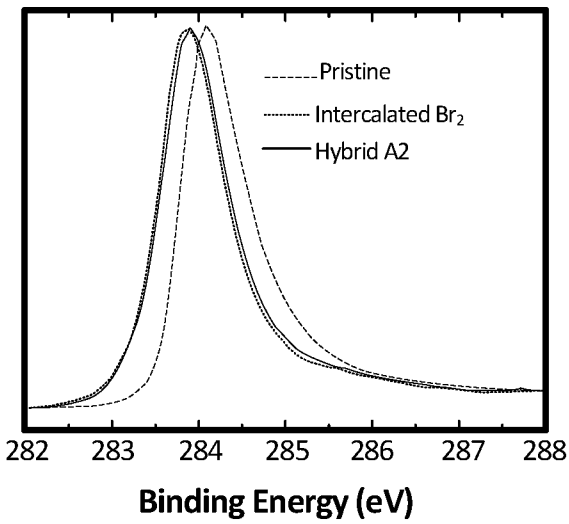


FIG. 3D

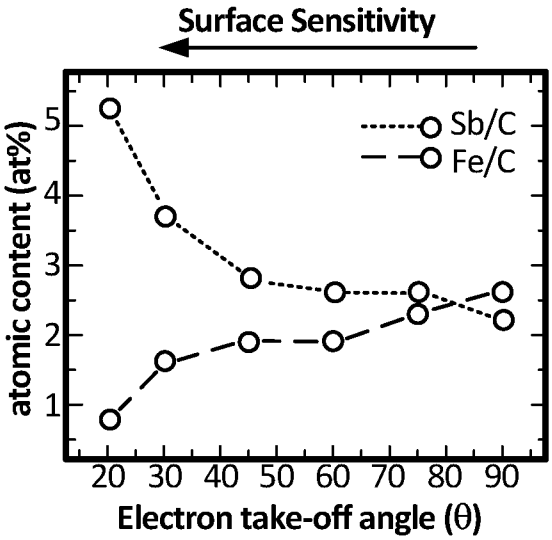


FIG. 4A

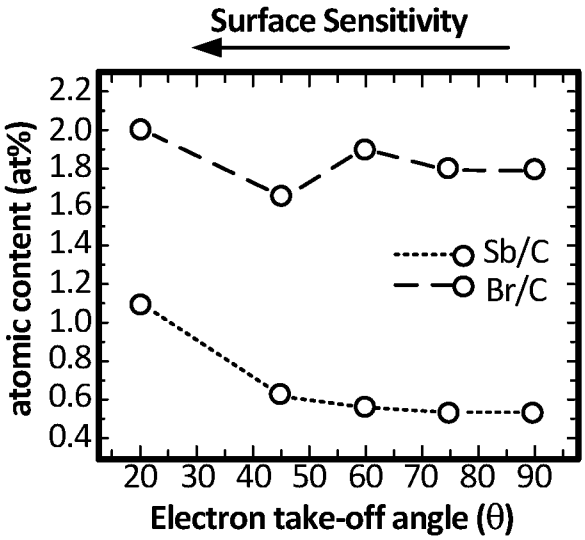


FIG. 4B

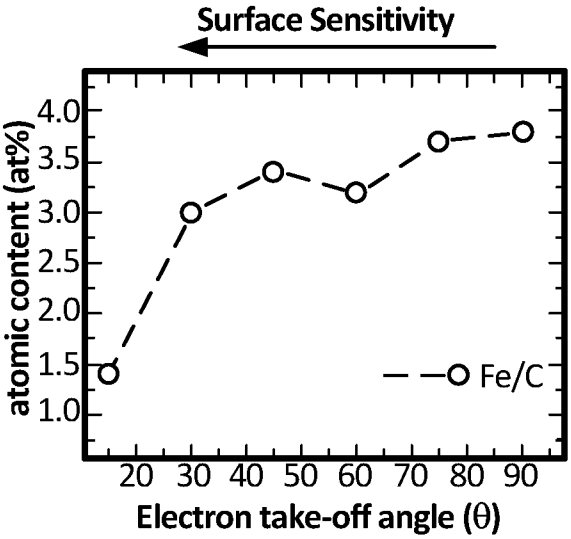


FIG. 4C

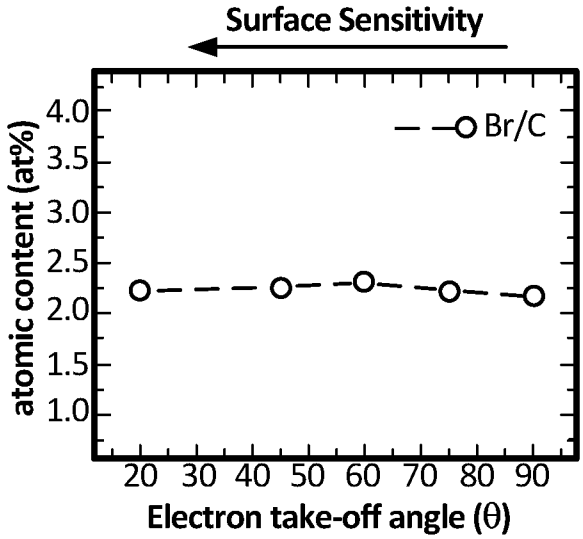


FIG. 4D

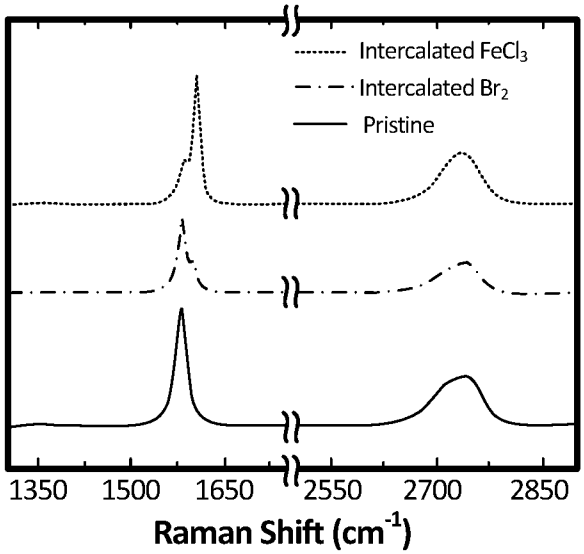


FIG. 5A

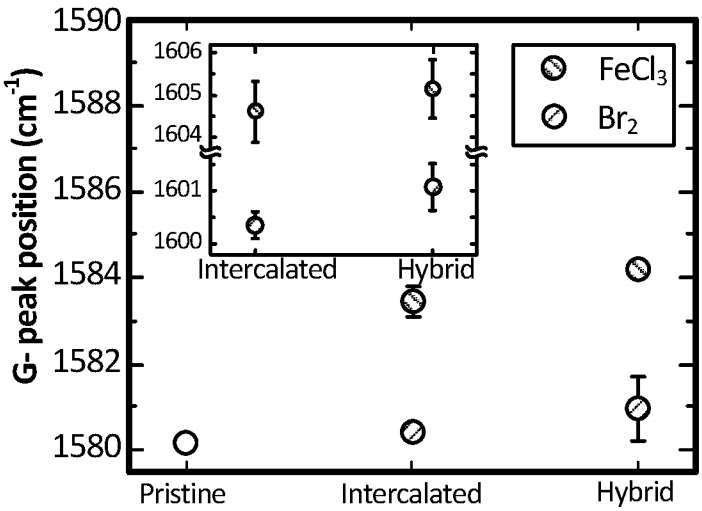


FIG. 5B

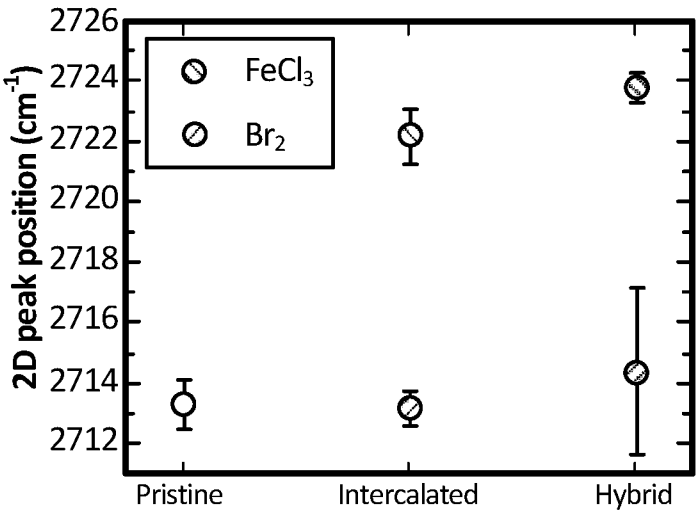


FIG. 5C

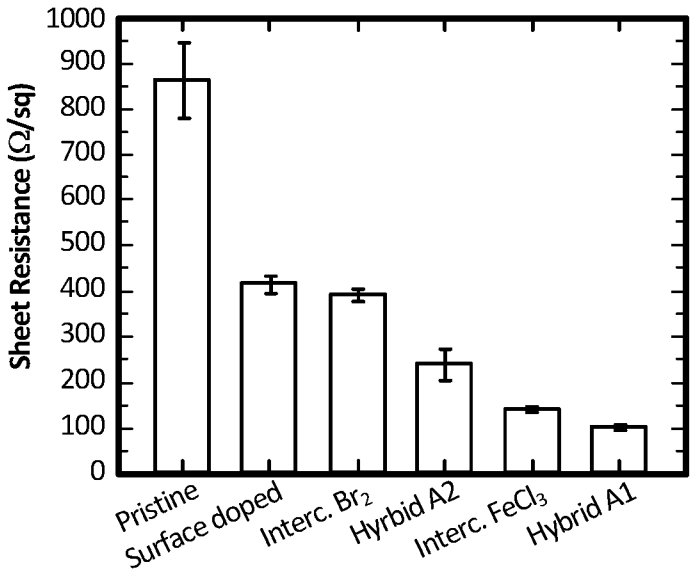


FIG. 6A

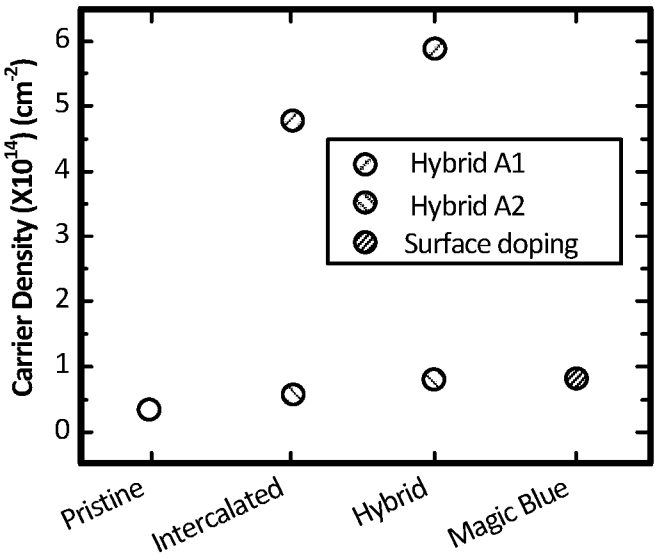


FIG. 6B

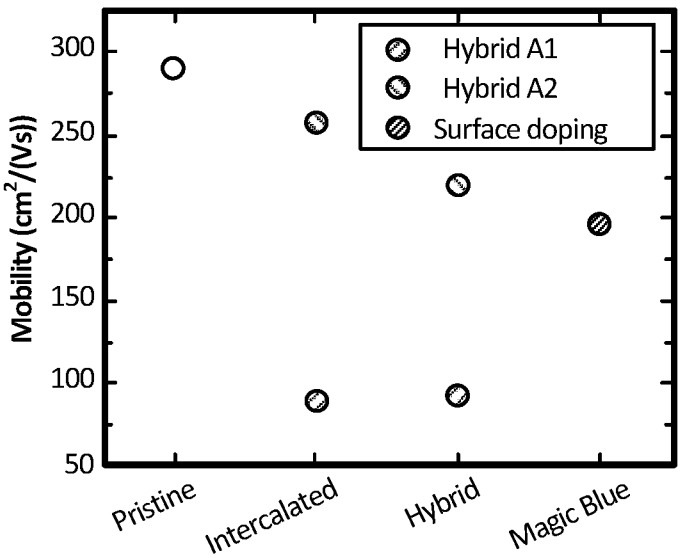


FIG. 6C

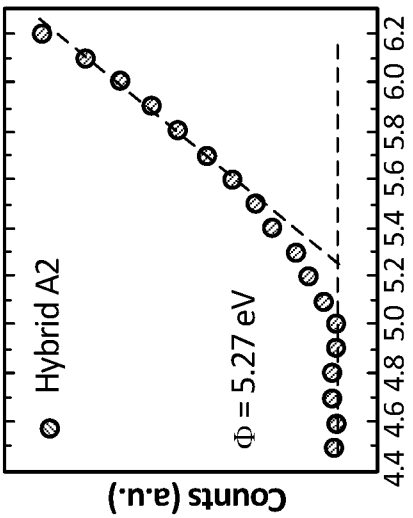


FIG. 7C

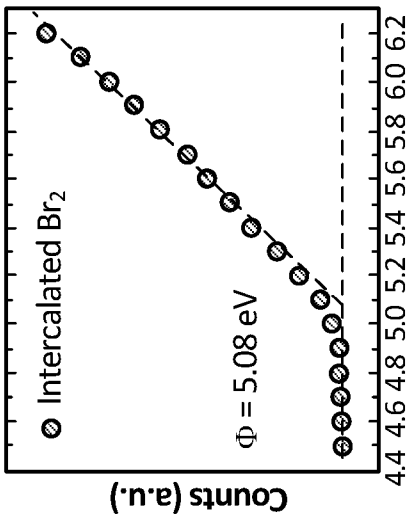


FIG. 7B

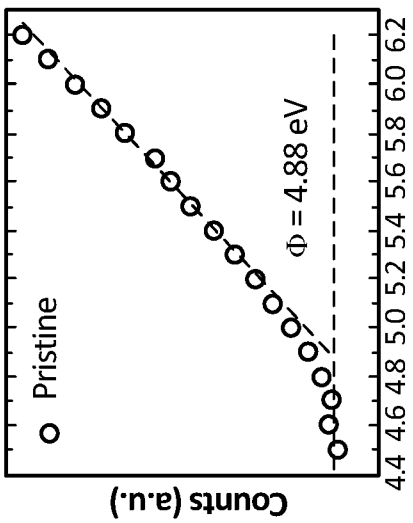


FIG. 7A

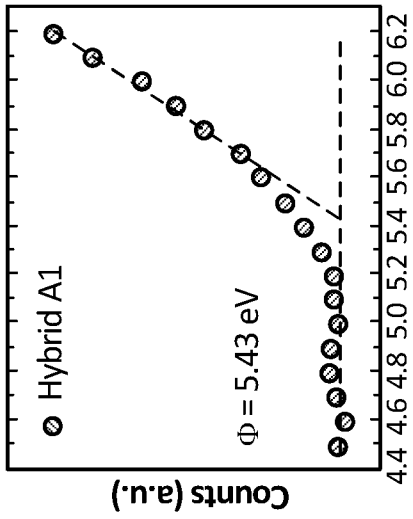


FIG. 7F

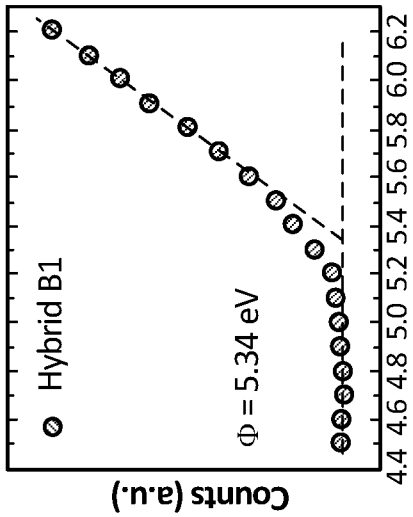


FIG. 7E

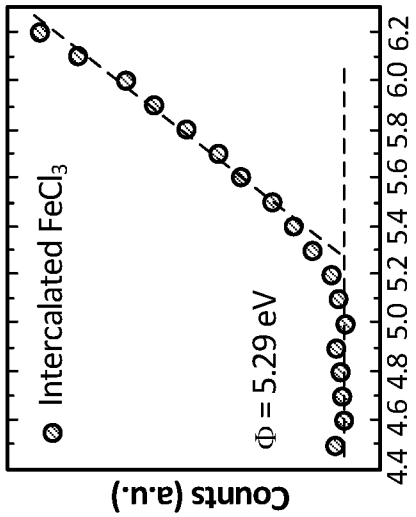


FIG. 7D

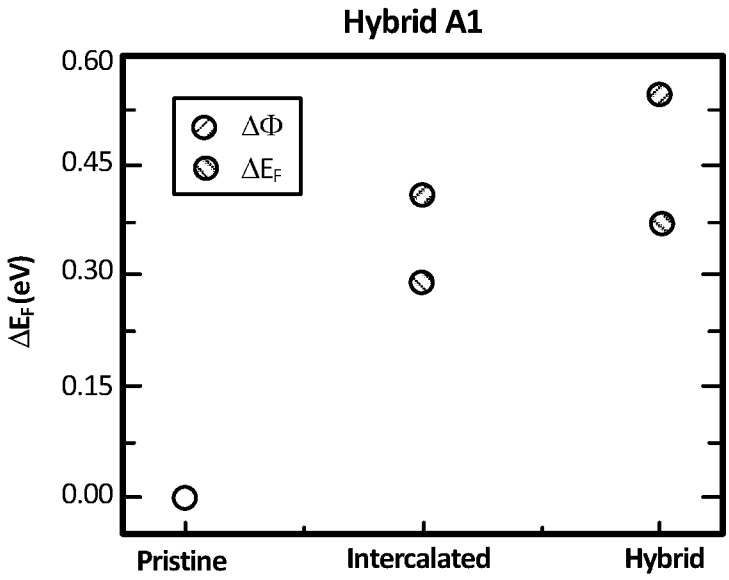

Hybrid A1
0.60
0.45
0.30
0.15
0.00
ΔE_F (eV)
ΔΦ
ΔE_F
Pristine
Intercalated
Hybrid

FIG. 8A

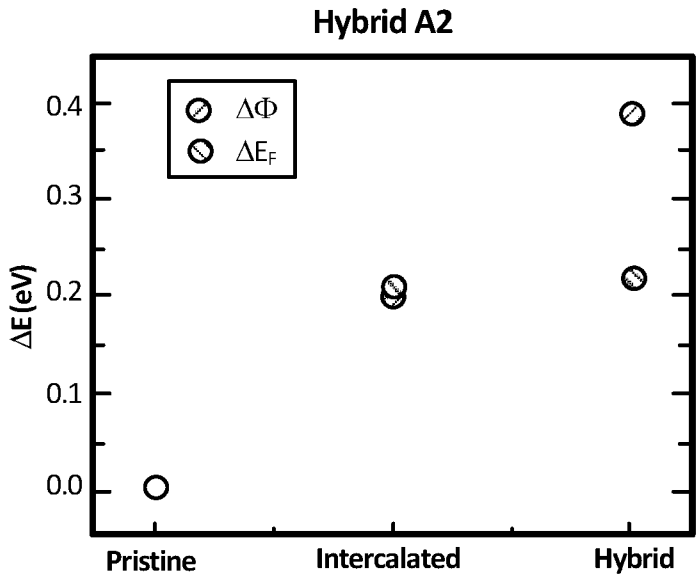

Hybrid A2
0.4
0.3
0.2
0.1
0.0
ΔE (eV)
ΔΦ
ΔE_F
Pristine
Intercalated
Hybrid

FIG. 8B

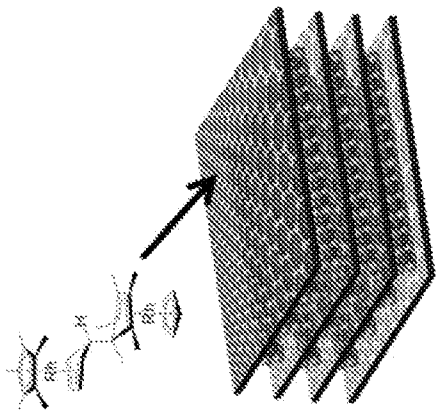


FIG. 9A

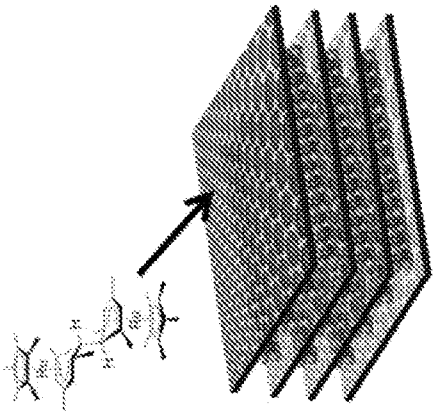


FIG. 9B

FIG. 9C

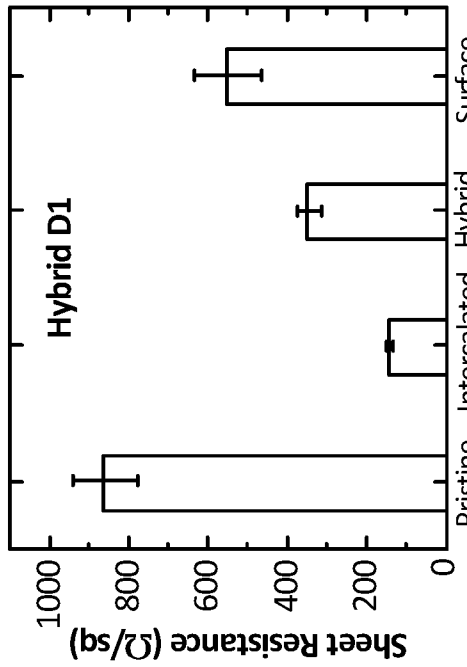


FIG. 9D

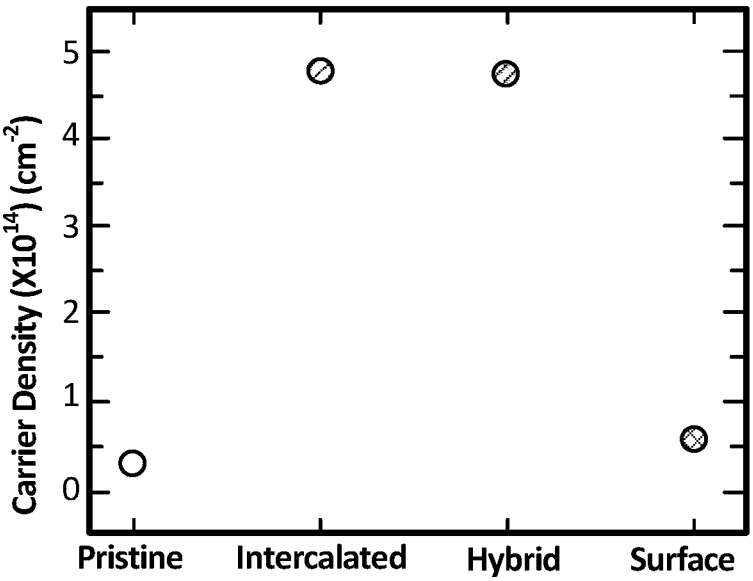


FIG. 10A

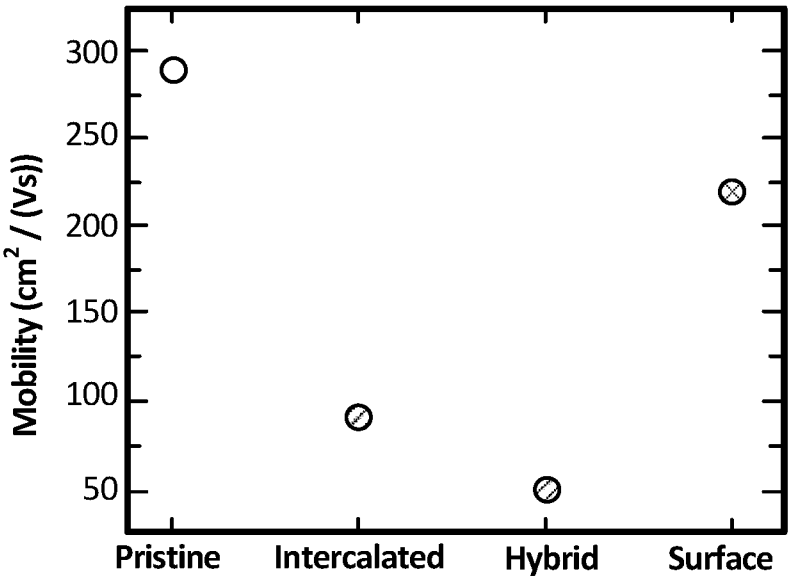


FIG. 10B

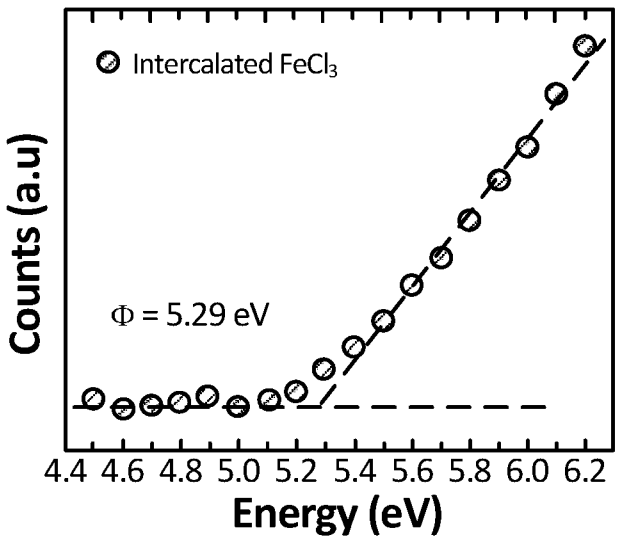


FIG. 11A

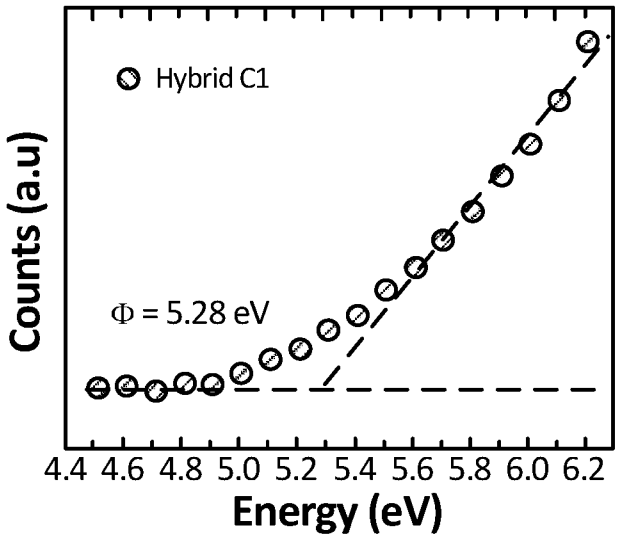


FIG. 11B

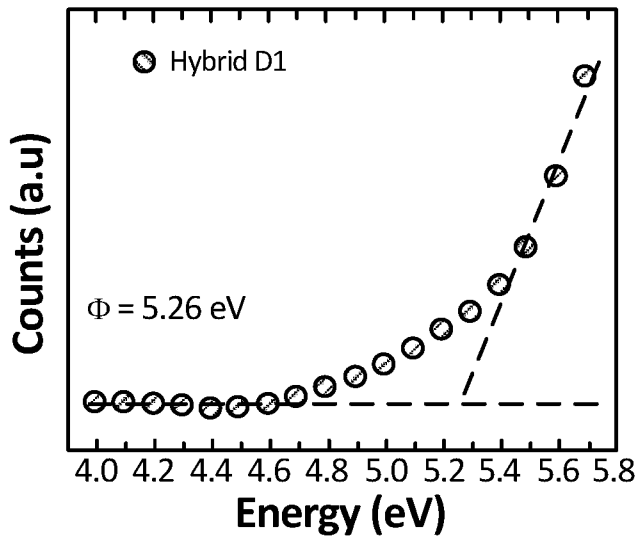


FIG. 11C

INTERNATIONAL SEARCH REPORT

International application No
PCT/IB2017/056577

A. CLASSIFICATION OF SUBJECT MATTER
INV. C01B32/22 C01B32/194
ADD.

According to International Patent Classification (IPC) or to both national classification and IPC

B. FIELDS SEARCHED

Minimum documentation searched (classification system followed by classification symbols)
B82Y H01B H01L C01B

Documentation searched other than minimum documentation to the extent that such documents are included in the fields searched

Electronic data base consulted during the international search (name of data base and, where practicable, search terms used)

EPO-Internal, WPI Data

C. DOCUMENTS CONSIDERED TO BE RELEVANT

Category*	Citation of document, with indication, where appropriate, of the relevant passages	Relevant to claim No.
X	US 2015/364614 A1 (WITHERS FREDDIE [GB] ET AL) 17 December 2015 (2015-12-17) paragraphs [0030] - [0031]	1-20
A	US 2005/075245 A1 (GODDARD WILLIAM A [US] ET AL) 7 April 2005 (2005-04-07) figure all	1-20
A	US 2014/174513 A1 (RUSSO SAVERIO [GB] ET AL) 26 June 2014 (2014-06-26) claim all	1-20
A	US 2013/048339 A1 (TOUR JAMES M [US] ET AL) 28 February 2013 (2013-02-28) claim all	1-20

☐ Further documents are listed in the continuation of Box C.

☒ See patent family annex.

* Special categories of cited documents :

"A" document defining the general state of the art which is not considered to be of particular relevance

"E" earlier application or patent but published on or after the international filing date

"L" document which may throw doubts on priority claim(s) or which is cited to establish the publication date of another citation or other special reason (as specified)

"O" document referring to an oral disclosure, use, exhibition or other means

"P" document published prior to the international filing date but later than the priority date claimed

"T" later document published after the international filing date or priority date and not in conflict with the application but cited to understand the principle or theory underlying the invention

"X" document of particular relevance; the claimed invention cannot be considered novel or cannot be considered to involve an inventive step when the document is taken alone

"Y" document of particular relevance; the claimed invention cannot be considered to involve an inventive step when the document is combined with one or more other such documents, such combination being obvious to a person skilled in the art

"&" document member of the same patent family

Date of the actual completion of the international search	Date of mailing of the international search report
30 January 2018	06/02/2018

Name and mailing address of the ISA/	Authorized officer
European Patent Office, P.B. 5818 Patentlaan 2 NL - 2280 HV Rijswijk Tel. (+31-70) 340-2040, Fax: (+31-70) 340-3016	Mattheis, Chris

1

INTERNATIONAL SEARCH REPORT

Information on patent family members

International application No
PCT/IB2017/056577

Patent document cited in search report	Publication date	Patent family member(s)	Publication date
US 2015364614 A1	17-12-2015	EP 2946407 A2	25-11-2015
		US 2015364614 A1	17-12-2015
		WO 2014111702 A2	24-07-2014
US 2005075245 A1	07-04-2005	AU 2003294429 A1	18-06-2004
		US 2005075245 A1	07-04-2005
		WO 2004048259 A1	10-06-2004
US 2014174513 A1	26-06-2014	NONE	
US 2013048339 A1	28-02-2013	CN 103038835 A	10-04-2013
		EP 2545561 A1	16-01-2013
		JP 2013542546 A	21-11-2013
		KR 20130038836 A	18-04-2013
		SG 183997 A1	30-10-2012
		US 2013048339 A1	28-02-2013
		WO 2011112589 A1	15-09-2011
		WO 2011112598 A1	15-09-2011